



Supplement of

Air quality and related health impact in the UNECE region: source attribution and scenario analysis

Claudio A. Belis and Rita Van Dingenen

Correspondence to: Claudio A. Belis (claudio.belis@ec.europa.eu)

The copyright of individual parts of the supplement might differ from the article licence.

Supplement

1 The TM5-FASST model

Linearized emission-concentration responses:

We use the reduced-form TM5-FASST air quality model (Van Dingenen et al., 2018) to compute global PM2.5 and ozone concentration grid maps for the selected scenarios of dietary change. TM5-FASST is built on linearized region-to-grid emission-concentration response fields that have been precomputed with the TM5 2-way nested global Chemistry-Transport Model (Krol et al., 2005), based on a 20% emission perturbation of a reference pollutant emission set (RCP year 2000) in each of 56 defined source regions. ‘Region-to-grid’ means that emissions are given as model input as regional totals (with implied and fixed spatial distribution for each source region) while the resulting pollutant concentrations are obtained as 1°x1° resolution grid maps.

For each 1°x1° grid cell, the change in concentration of component j in receptor y resulting from a -20% emission perturbation of precursor i in all grid cells of source region x , is expressed by a unique source-receptor (SR) coefficient $A_{ij}[x, y]$:

$$A_{ij}[x, y] = \frac{\Delta C_j(y)}{\Delta E_i(x)} \text{ with } \Delta E_i(x) = 0.2 E_{i,\text{ref}}(x) \quad \text{Eq. S1}$$

The total concentration of a component (or metric) j in receptor region y , resulting from emissions of *all* n_i precursors i at *all* n_x source regions x , is obtained as a ‘perturbation’ on the reference-simulation concentration, by summing up all the respective SR coefficients scaled with the actual emission ‘perturbation’, being the difference between the reference and actual emission:

$$C_j(y) = C_{j,\text{ref}}(y) + \Delta C_j(y) \quad \text{Eq. S2}$$

$$\Delta C_j(y) = \sum_{k=1}^{n_x} \sum_{i=1}^{n_i} A_{ij}[x_k, y] \cdot [E_i(x_k) - E_{i,\text{ref}}(x_k)] \quad \text{Eq. S3}$$

$C_{j,\text{ref}}(y)$, $A_{ij}[x_k, y]$ and $E_{i,\text{ref}}(x_k)$ are fixed and have been determined ‘once and for all’ using the RCP year 2000 reference TM5 run and the 20% emission perturbations on the latter. The only scenario-dependent input is $E_i(x_k)$, i.e. the actual scenario emission for the considered pollutant, aggregated over the source region.

Pollutants C_j include particulate matter components (SO₄, NO₃, NH₄, BC, particulate organic matter – POM), trace gases (SO₂, NO, NO₂, NH₃, O₃), and deposition fluxes of BC, N and S species. In the case of ozone, the n_i precursors in the above equation comprise [NO_x, NMVOC, CO, CH₄].

Sub-grid downscaling for primary PM2.5:

A parameterization of the urban increment for (non-reactive) primary emitted anthropogenic black carbon and organic matter has been implemented by scaling the sub-grid emission strength of those compounds to urban and rural sub-grids within the native grid cell.

This is accomplished using a high-resolution (2.5'x2.5') population dataset (CIESIN, university of Columbia) which subdivides the 1°x1° native grid in 24x24 subgrids. A subgrid is labelled as 'urban' if the population density exceeds 600/km², and 'rural' otherwise.

Let f_{UP} be the urban population fraction, defined as the fraction of the population within the 1°x1° gridcell which resides in the urban-flagged subgrids, and f_{UA} the urban area fraction, being the fraction of the 1x1 grid area occupied by the urban-flagged subgrids (in practice: the number of urban subgrids divided by 576, i.e. the total nr. of subgrids).

Let E_{BC} be the emission strength of the anthropogenic BC of the whole native grid cell. We make the assumption that the fraction $f_{UP} \cdot E_{BC}$ is emitted from area $f_{UA} \cdot A$ (A being the grid cell area) and $(1 - f_{UP}) \cdot E_{BC}$ from area $(1 - f_{UA}) \cdot A$.

Under steady-state conditions, neglecting the incoming concentration of BC from neighbouring gridcells, the 1°x1° grid-average BC concentration can be written as:

$$C_{BC,1x1} = \frac{E_{BC}}{\lambda} \text{ with } \lambda = \text{ventilation factor} \quad \text{Eq S4}$$

Assuming the ventilation factor λ is also valid for the urban and rural part of the grid cell (equivalent with the assumption that mixing layer height and wind speed are the same), the steady-state concentration in the urban sub-area can be written as:

$$C_{BC} = \frac{f_{UP}}{f_{UA}} \frac{E_{BC}}{\lambda} \text{ and } C_{BC} = \frac{(1 - f_{UP})}{(1 - f_{UA})} \frac{E_{BC}}{\lambda} \quad \text{Eq S5}$$

The ventilation factor, including an implicit correction factor for the non-zero background concentration in neighbouring cells, is obtained by taking advantage of the explicitly modelled gridcell concentration with the chemical transport model (C_{TM5}):

$$\lambda = \frac{E_{BC}}{C_{BC,TM5}} \quad \text{Eq S6}$$

Hence,

$$C_{BC,URB} = \frac{f_{UP}}{f_{UA}} C_{BC,TM5} \text{ and } C_{BC,RUR} = \frac{(1 - f_{UP})}{(1 - f_{UA})} C_{BC,TM5} \quad \text{Eq S7}$$

To avoid artificial spikes in urban concentrations when occasionally a very small fraction of the native grid cell contains a very large fraction of the population, we apply empirical bounds on the adjustment factors:

Rural Primary BC and POM ($C_{eq,RUR}$) should not be lower than 0.5 times the TM5 grid average

Urban primary BC and POM should not exceed the rural concentration by a factor of 5.

In any case, the urban and rural adjustments for each of the primary components must fulfil the condition:

$$f_{UA}C_{URB} + (1 - f_{UA})C_{RUR} = C_{TM5} \quad \text{Eq S8}$$

The adjusted urban and rural concentrations of the primary emitted components can be cast in one 1°x1°-grid population-weighted average value:

$$C_{BC,TM5}^{pop} = f_{UP} \cdot C_{BC,URB} + (1 - f_{UP}) \cdot C_{BC,RUR} \quad \text{Eq S9}$$

After substituting $C_{BC,URB}$ and $C_{BC,RUR}$, the population-weighted concentration is expressed as a function of the area-weighted average concentration:

$$C_{BC,TM5}^{pop} = \left[\frac{(f_{UP})^2}{f_{UA}} + \frac{(1 - f_{UP})^2}{1 - f_{UA}} \right] \cdot C_{BC,TM5}^{area} \quad \text{Eq S10}$$

And similar for primary anthropogenic organic carbon.

All secondary components (sulfates, nitrates) and primary natural PM (mineral dust, sea salt) are assumed to be distributed uniformly over the native 1x1 gridcell.

CH₄ – Ozone interactions:

The spatial explicit surface level O₃ response to changing CH₄ concentration for the year 2000 is embedded in a single gridded global response field (fig. S1), representing the response to a reduction of the global CH₄ concentration of 20%. CH₄ affects ozone both in the free troposphere and in the boundary layer. The highest O₃ response to CH₄ emission changes are observed where free tropospheric downwelling occurs frequently and where the local O₃ formation regime is VOC-limited (West and Fiore, 2005; Fiore et al., 2008).

To avoid expensive transient computations, prescribed fixed CH₄ concentrations (1760 ppb and 1408 ppb, see Dentener et al., 2010) were used in the full CTM TM5 to establish CH₄ – O₃ response sensitivities. Previous transient modeling studies have shown that a change in steady-state CH₄ abundance can be traced back to a sustained change in emissions, but the relation is not linear because an increase in CH₄ emissions removes an additional fraction of atmospheric OH (the major sink for CH₄) and prolongs the lifetime of CH₄ (Fiore et al., 2002, 2008; Prather et al., 2001). In a steady-state situation, the CH₄ concentration is the result of balanced sources and sinks. Keeping all other emissions constant, the change in the amount of CH₄ loss (mainly by OH oxidation with a lifetime of ca. 9 years, neglecting loss to soils and stratosphere with lifetimes of ca.160 and 120 years respectively (Prather et al., 2001)) under the prescribed change in CH₄ abundance should therefore be balanced by an equal and opposite source which we consider as an “effective emission”. The amount of CH₄ oxidized by OH in one year being diagnosed by the model, the resulting difference between the reference and perturbation experiment of -77 Tg sets the balancing “effective” emission rate to 77Tg/yr, which is then used to express the resulting O₃ and O₃ metrics response as a function of a CH₄ *emission* change.

The ozone-CH₄ responses applied in the present study assume an immediate impact and neglect the time lag between CH₄ emission change and new steady state (12 year lifetime), which is also the approach taken in previous studies based on reduced-form models (e.g. Wild et al., 2012, Turnock et al., 2018).

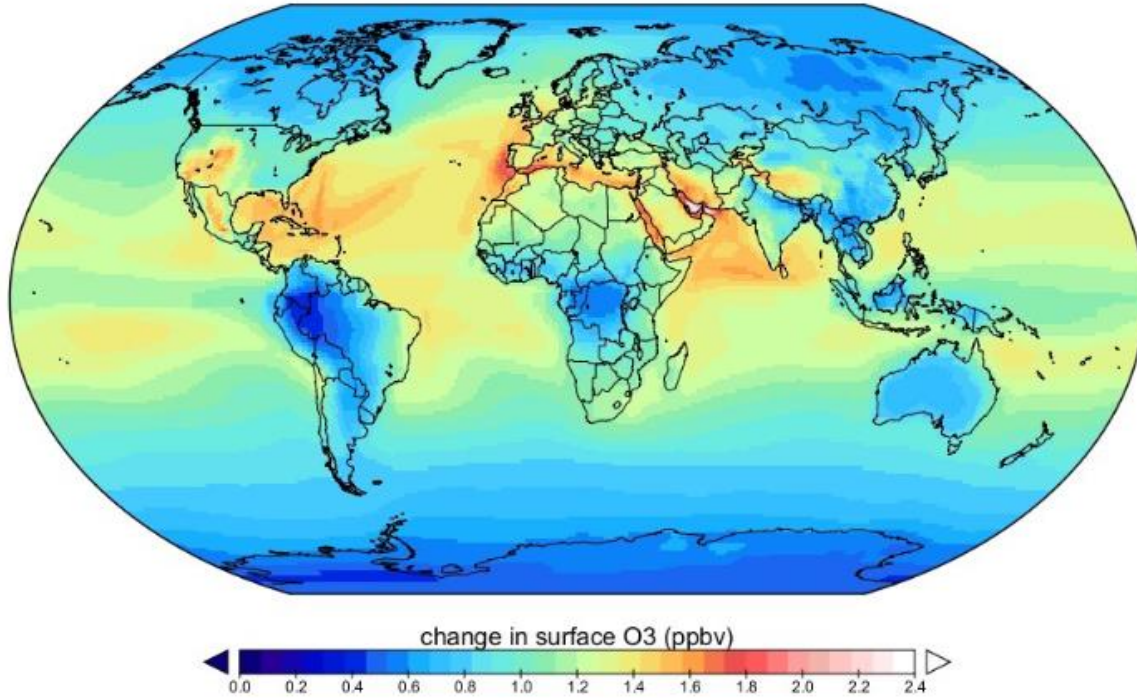


Figure S1. Steady-state decrease in annual mean surface O₃ for a 20% decrease in year 2000 CH₄ concentration, corresponding to a sustained 77Tg/yr CH₄ emission decrease.

Health impact assessment methodology

Population weighted annual mean PM_{2.5} at 35% relative humidity and seasonal daily maximum 8h average O₃ concentration metric (SDMA8h) are the exposure metrics used to compute health impacts in line with epidemiological studies (Jerrett et al., 2009; Krewski et al., 2009; Pope III et al., 2002). Mortality associated with PM_{2.5} is calculated, using the integrated exposure-response model (IER) adopted in the Global Burden of Disease (GBD2017) assessment (Stanaway et al., 2018), as the number of annual premature mortalities from six causes of death: chronic obstructive pulmonary disease (COPD), lung cancer (LC), lower respiratory airway infections (LRI), type 2 diabetes mellitus (DM), ischemic heart disease (IHD), and stroke.

Cause-specific excess mortalities are calculated at grid cell level using a population-attributable fraction approach (Murray et al., 2003):

$$\Delta Mort = m_0 \cdot AF \cdot POP \quad (1)$$

$$AF = \frac{(RR-1)}{RR} \quad (2)$$

where m_0 is the baseline mortality rate (deaths per capita) for the exposed population POP, AF is the fraction of total mortalities attributable to air pollution, and RR is the relative risk of death attributable to

a change in P.W. mean pollutant concentration. For $PM_{2.5}$ exposure, RR is derived from the IER functions (Burnett et al., 2014):

$$RR_{PM_{2.5}} = 1 + \alpha \{1 - \exp[-\gamma(PM_{2.5} - zcf)^\delta]\} \text{ for } PM_{2.5} > zcf \quad (3)$$
$$RR_{PM_{2.5}} = 1 \quad \text{for } PM_{2.5} \leq zcf$$

where α , γ and δ are parameters provided in the abovementioned references and zcf is the counterfactual concentration, i.e. a theoretical minimum exposure level below which there is no excess risk. α , γ , δ , and zcf were obtained from fittings to the median and 95 percentile exposure response curves of 1000 sampled RR 's in the exposure range 1 – 600 $\mu\text{g}/\text{m}^3$. Our fittings reproduce the IER functions applied in the Global Burden of Disease 2017 assessment (Stanaway et al., 2018).

Mortality attributable to ozone exposure is based on the log-linear exposure-response function following the GBD approach, using the SDMA8h indicator with a RR of 1.06/10 ppb for COPD and a zero-risk threshold (zcf) of 29.1 ppb (Van Dingenen et al., 2018; Belis et al., 2022).

Bibliography

Belis, C. A., Van Dingenen, R., Klimont, Z., and Dentener, F.: Scenario analysis of $PM_{2.5}$ and ozone impacts on health, crops and climate with TM5-FASST: A case study in the Western Balkans, *Journal of Environmental Management*, 319, 115738, <https://doi.org/10.1016/j.jenvman.2022.115738>, 2022.

Burnett Richard, T., Pope, C. A., Ezzati, M., Olives, C., Lim Stephen, S., Mehta, S., Shin Hwashin, H., Singh, G., Hubbell, B., Brauer, M., Anderson, H. R., Smith Kirk, R., Balmes John, R., Bruce Nigel, G., Kan, H., Laden, F., Prüss-Ustün, A., Turner Michelle, C., Gapstur Susan, M., Diver, W. R., and Cohen, A.: An Integrated Risk Function for Estimating the Global Burden of Disease Attributable to Ambient Fine Particulate Matter Exposure, *Environmental Health Perspectives*, 122, 397-403, 10.1289/ehp.1307049, 2014.

Dentener, F., Keating, T., Akimoto, H., Pirrone, N., Dutchak, S., Zuber, A., Convention on Long-range Transboundary Air Pollution, United Nations, and UNECE Task Force on Emission Inventories and Projections (Eds.): Hemispheric transport of air pollution 2010: prepared by the Task Force on Hemispheric Transport of Air Pollution acting within the framework of the Convention on Long-range Transboundary Air Pollution, United Nations, New York ; Geneva, 4 pp., 2010.

Fiore, A. M., Jacob, D. J., Field, B. D., Streets, D. G., Fernandes, S. D., and Jang, C.: Linking ozone pollution and climate change: The case for controlling methane, *Geophysical Research Letters*, 29, 25-1-25-4, <https://doi.org/10.1029/2002GL015601>, 2002.

Fiore, A. M., West, J. J., Horowitz, L. W., Naik, V., and Schwarzkopf, M. D.: Characterizing the tropospheric ozone response to methane emission controls and the benefits to climate and air quality, *Journal of Geophysical Research Atmospheres*, 113, <https://doi.org/10.1029/2007JD009162>, 2008.

Fiore, A. M., Dentener, F. J., Wild, O., Cuvelier, C., Schultz, M. G., Hess, P., Textor, C., Schulz, M., Doherty, R. M., Horowitz, L. W., MacKenzie, I. A., Sanderson, M. G., Shindell, D. T., Stevenson, D. S., Szopa, S., Van Dingenen, R., Zeng, G., Atherton, C., Bergmann, D., Bey, I., Carmichael, G., Collins, W. J., Duncan, B. N., Faluvegi, G., Folberth, G., Gauss, M., Gong, S., Hauglustaine, D., Holloway, T., Isaksen, I. S. A., Jacob, D. J., Jonson, J. E., Kaminski, J. W., Keating, T. J., Lupu, A., Marmer, E., Montanaro, V., Park, R. J., Pitari, G., Pringle, K. J., Pyle, J. A., Schroeder, S., Vivanco, M. G., Wind, P., Wojcik, G., Wu, S., and Zuber, A.: Multimodel estimates of intercontinental source-receptor relationships for ozone pollution, *Journal of Geophysical Research: Atmospheres*, 114, <https://doi.org/10.1029/2008JD010816>, 2009.

Jerrett, M., Burnett, R. T., Pope, C. A., Ito, K., Thurston, G., Krewski, D., Shi, Y., Calle, E., and Thun, M.: Long-Term Ozone Exposure and Mortality, *New England Journal of Medicine*, 360, 1085-1095, 10.1056/NEJMoa0803894, 2009.

Krewski, D., Jerrett, M., Burnett, R. T., Ma, R., Hughes, E., and Shi, Y., : Extended Follow-Up and Spatial Analysis of the American Cancer Society Study Linking Particulate Air Pollution and Mortality, Health Effects Institute, Boston, USA, 2009.

Krol, M., Houweling, S., Bregman, B., van den Broek, M., Segers, A., van Velthoven, P., Peters, W., Dentener, F., and Bergamaschi, P.: The two-way nested global chemistry-transport zoom model TM5: algorithm and applications, *Atmos. Chem. Phys.*, 5, 417-432, 10.5194/acp-5-417-2005, 2005.

Murray, C. J. L., Ezzati, M., Lopez, A. D., Rodgers, A., and Vander Hoorn, S.: Comparative quantification of health risks: Conceptual framework and methodological issues, *Population Health Metrics*, 1, 1, 10.1186/1478-7954-1-1, 2003.

Pope III, C. A., Burnett, R. T., Thun, M. J., Calle, E. E., Krewski, D., Ito, K., and Thurston, G. D.: Lung Cancer, Cardiopulmonary Mortality, and Long-term Exposure to Fine Particulate Air Pollution, *JAMA*, 287, 1132-1141, 10.1001/jama.287.9.1132, 2002.

Prather, M., Ehhalt, D., Dentener, F., Derwent, R., Dlugokencky, E., Holland, E., Isaksen, I., Katima, J., Kirchhoff, V., Matson, P., Midgley, P., Wang, M., Bernsten, T., Bey, I., Brasseur, G., Buja, L., Pitari, G., and Et, A.: Chapter 4: Atmospheric Chemistry and Greenhouse Gases, Cambridge University Press, 2001.

Stanaway, J. D., Afshin, A., Gakidou et al., C. J. L.: Global, regional, and national comparative risk assessment of 84 behavioural, environmental and occupational, and metabolic risks or clusters of risks for 195 countries and territories, 1990–2017: a systematic analysis for the Global Burden of Disease Study 2017, *The Lancet*, 392, 1923-1994, [https://doi.org/10.1016/S0140-6736\(18\)32225-6](https://doi.org/10.1016/S0140-6736(18)32225-6), 2018.

Turnock, S. T., Wild, O., Dentener, F. J., Davila, Y., Emmons, L. K., Flemming, J., Folberth, G. A., Henze, D. K., Jonson, J. E., Keating, T. J., Kengo, S., Lin, M., Lund, M., Tilmes, S., and O'Connor, F. M.: The impact of future emission policies on tropospheric ozone using a parameterised approach, *Atmospheric Chemistry and Physics*, 18, 8953–8978, <https://doi.org/10.5194/acp-18-8953-2018>, 2018.

Van Dingenen, R., Dentener, F., Crippa, M., Leita, J., Marmer, E., Rao, S., Solazzo, E., and Valentini, L.: TM5-FASST: a global atmospheric source–receptor model for rapid impact analysis of emission changes on air quality and short-lived climate pollutants, *Atmos. Chem. Phys.*, 18, 16173-16211, 10.5194/acp-18-16173-2018, 2018.

West, J. J. and Fiore, A. M.: Management of Tropospheric Ozone by Reducing Methane Emissions, *Environmental Science & Technology*, 39, 4685–4691, <https://doi.org/10.1021/es048629f>, 2005.

Wild, O., Fiore, A. M., Shindell, D. T., Doherty, R. M., Collins, W. J., Dentener, F. J., Schultz, M. G., Gong, S., MacKenzie, I. A., Zeng, G., Hess, P., Duncan, B. N., Bergmann, D. J., Szopa, S., Jonson, J. E., Keating, T. J., and Zuber, A.: Modelling future changes in surface ozone: a parameterized approach, *Atmospheric Chemistry and Physics*, 12, 2037–2054, <https://doi.org/10.5194/acp-12-2037-2012>, 2012.

4 Source apportionment of O₃ exposure in three Eclipse v6b scenarios.

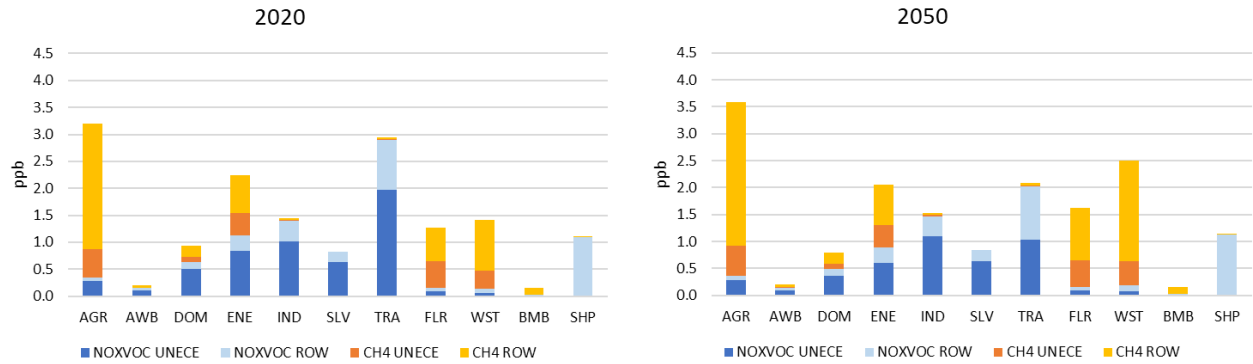


Figure S3. Apportionment of O₃ exposure to its anthropogenic sources in the CLC scenario in 2020 and 2050.

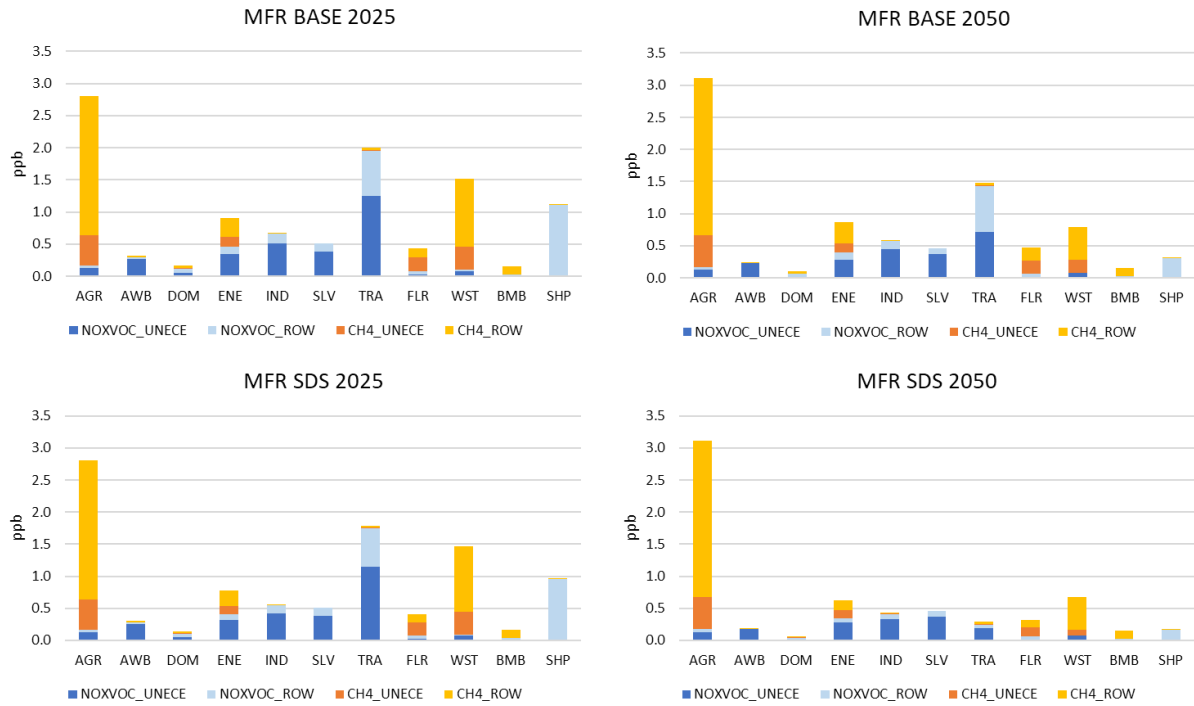


Figure S4. Apportionment of O₃ exposure to its anthropogenic sources in the MFR BASE and MFR-SDS scenarios in 2025 and 2050.